Supporting Information for

One-pot mechanochemical synthesis to encapsulate functional guests into a metal-organic framework for proton conduction

Yang Wang, Ying Lu,* Zhuo Li, Xiu-Wei Sun, Wan-Yu Zhang, Shan Zhang, Jie Wang, Tian-Yi Dang, Zhong Zhang and Shu-Xia Liu*

Key Laboratory of Polyoxometalate and Reticular Material Chemistry of the Ministry of Education,

College of Chemistry, Northeast Normal University,

Changchun, Jilin 130024, China

*e-mail: liusx@nenu.edu.cn; luy968@nenu.edu.cn

Contents

Section S1 Experimental Section

1. Materials:

All the chemicals and reagents including cupric nitrate hydrate, trimesic acid, phosphotungstic acid, imidazole, urea, sulfamic acid and (Aminomethyl) phosphonic acid, sodium hydroxide, ethanol were obtained from commercial sources and used without further purification.

2. Instruments:

Elemental analyses (CHN) were conducted on a PerkinElmer 2400 CHN Elemental analyzer. Infrared (IR) spectroscopy was performed in the range of 4000-400 cm^{-1} using the KBr pellet on an Alpha Centaurt FT/IR spectrophotometer. The room temperature powder X-ray diffraction (PXRD) spectra in the range of 2θ = 5-50° were performed on a Siemens D5005 diffractometer with Cu-Kα radiation. X-ray photoelectron spectra (XPS) were collected on Thermo ESCALAB 250 X-ray photoelectron spectrometer. Thermal gravimetric analysis (TGA) was carried out using a Perkin-Elmer TG-7 analyzer in flowing N_2 heated from room temperature to 600 °C with a heating rate of 10 °C/min. The water adsorption and desorption isotherms of the complex 1' were carried out by ASAP 2020 instrument at 25 °C. The alternating current (AC) impedance spectroscopy data were obtained using a Solartron SI 1260 Impedance/Gain-Phase Analyzer over the frequency range of 10-10^7 Hz and an applied voltage of 200 mV.

3. Synthesis

Im@NENU-3:

$Cu(NO_3)_2{\cdot}3\,H_2O$ (0.24 g, 1 mmol) and $H_3PW_{12}O_{40}{\cdot}n\,H_2O$ (0.28 g, 0.092 mmol) were milled for 3 min in an agate mortar. Then H_3BTC (0.14 g, 0.67 mmol), imidazole (0.1 g, 0.15 mmol) and ethanol (0.7mL) were added to the mortar at ambient temperature and ground for 8 minutes to obtain blue solid material. The yielded product was washed several times with deionized water and ethanol, respectively. After drying in an oven at 60 °C for 24 h, the blue Im@NENU-3 was obtained in 95 % yield (calculated on the basis of Cu). Elemental and ICP analyses: C 16.97, H 1.92, N 2.58, P 0.49, Cu 12.16, W 34.87 %.

APA@NENU-3, Urea@NENU-3 and SA@NENU-3:

The synthesis method is similar to Im@NENU-3. Just replace imidazole with (Aminomethyl) phosphonic acid, urea, and sulfamic acid, respectively. Elemental and ICP analyses: APA@NENU-3 (C 14.64, H 1.62, N 1.64, P 4.07, Cu 11.78, W 33.72 %); Urea@NENU-3 (C 15.49, H 1.53, N 2.44, P 0.53, Cu 12.84, W 36.81 %); SA@NENU-3 (C 14.39, H 1.58, N 0.68, P 0.51, Cu 12.79, W 36.67 %).

NENU-3:

$Cu(NO_3)_2{\cdot}3\,H_2O$ (0.24 g, 1 mmol) and $H_3PW_{12}O_{40}{\cdot}n\,H_2O$ (0.28 g, 0.092 mmol) were milled for 3 min in an agate mortar. Then H_3BTC (0.14 g, 0.67 mmol) and ethanol (0.7mL) were added to the mortar at ambient temperature and ground for 5 minutes to obtain blue solid material. The yielded product was washed several times with deionized water and ethanol, respectively. Elemental and ICP analyses: C 12.68, H 1.85, P 0.51, Cu 12.68, W 36.40 %.

4. Proton Conductivities Studies

The compacted tablet used for conductivity measurements has a diameter of 0.8 cm and a thickness in the range of 0.05-0.06 cm, which was obtained by pressing crystal powders at 6 Mpa for 1 min. The tablet was sandwiched by two copper-plated electrodes. The changing temperature (298K-338K) and relative humidity environments (55 to 95% RH) were controlled by the Memmert HCP108 constant temperature humidity chamber. During the variable temperature/ RH conductivity measurement, samples were equilibrated for at least 2 hours after each step in temperature or 12 hours for each step in RH. The proton conductivities were calculated using the equation: $\sigma = L / (S \cdot R)$, where L and S are the thickness (cm) and cross-sectional area (cm^2) of the tablet, respectively. The σ is the proton conductivity ($S\ cm^{-1}$). The activation energy was calculated from the following Arrhenius equation:

$$\sigma T = \sigma_0 \exp(-Ea / k_B T)$$

Where σ is the proton conductivity, k_B is the Boltzmann constant, σ_0 is the pre-exponential factor, and T is the temperature.

Section S2 Additional Structural Figures and Characterizations

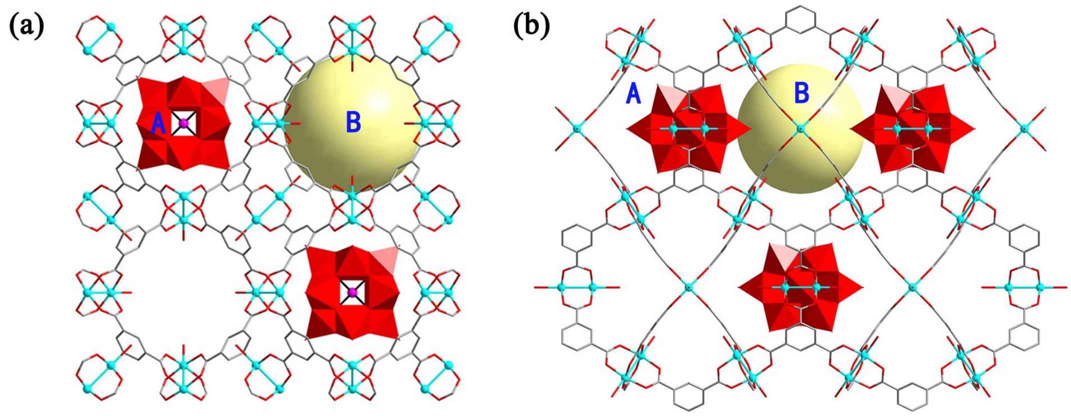

Fig. S1 The pore structure of NENU-3. (a) <100> orientation. (b) <110>orientation. P (pink), W (dark teal), Cu (sky blue), C (gray), O (red). All H atoms are omitted for clarity.

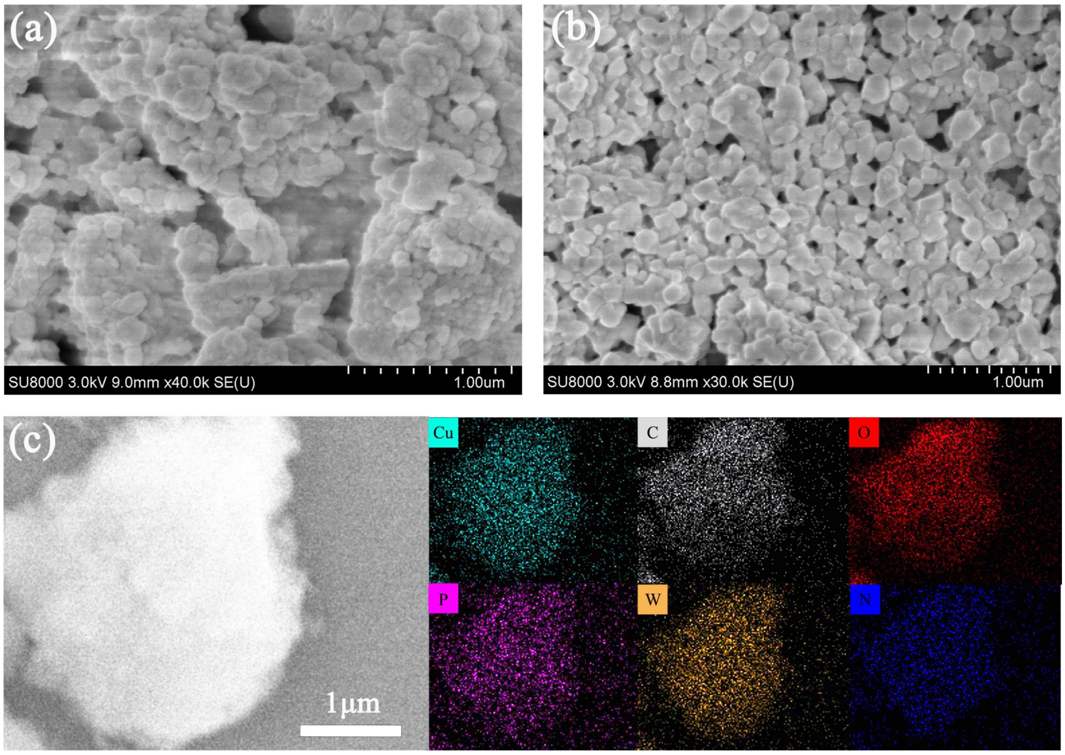

Fig. S2 SEM images of (a) NENU-3 and (b) Im@NENU-3, (c) SEM image and corresponding elemental mappings of Im@NENU-3.

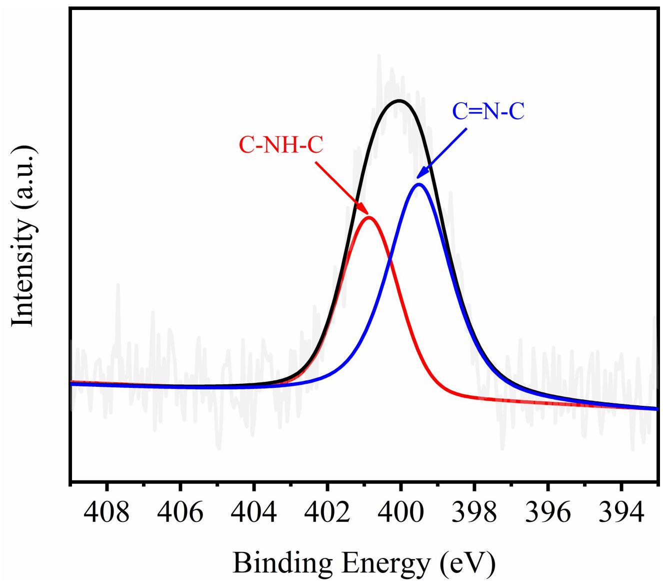

Fig. S3 Nitrogen 1s photoelectron spectroscopy for Im@NENU-3

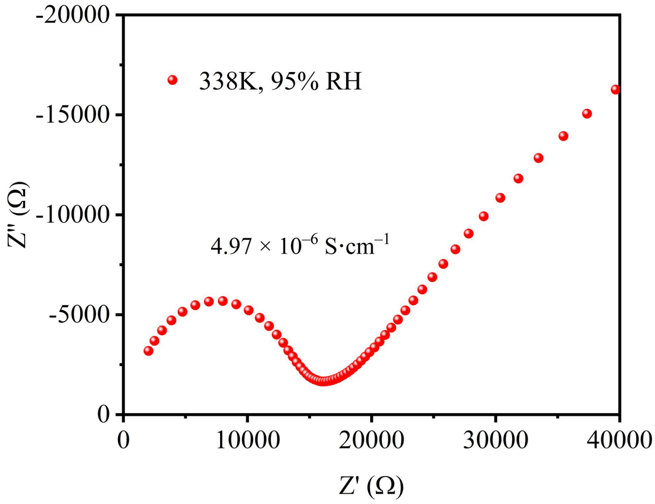

Fig. S4 Nyquist plot of NENU-3 at 95% RH and 338K.

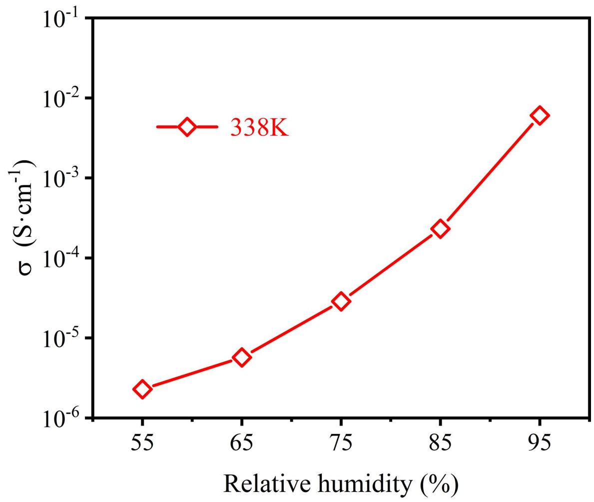

Fig. S5 Humidity dependence of proton conductivity at 338K for Im@NENU-3.

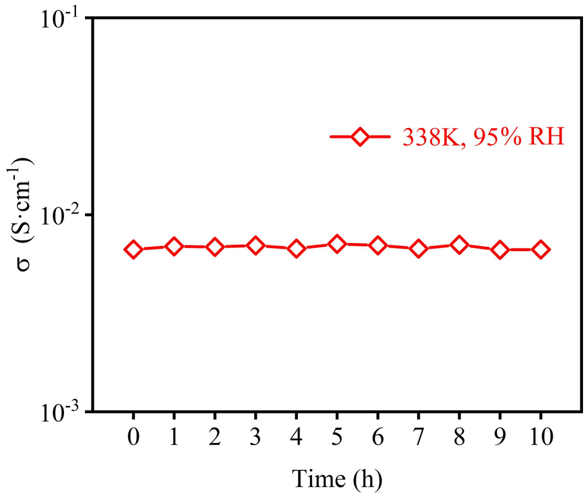

Fig. S6 Time-dependent proton conductivity of Im@NENU-3 at 338K and 95%RH

The high proton conductivity of Im@NENU-3 at 338K and 95%RH can maintain at least 10 h, so Im@NENU-3 possesses excellent proton-conducting durability.

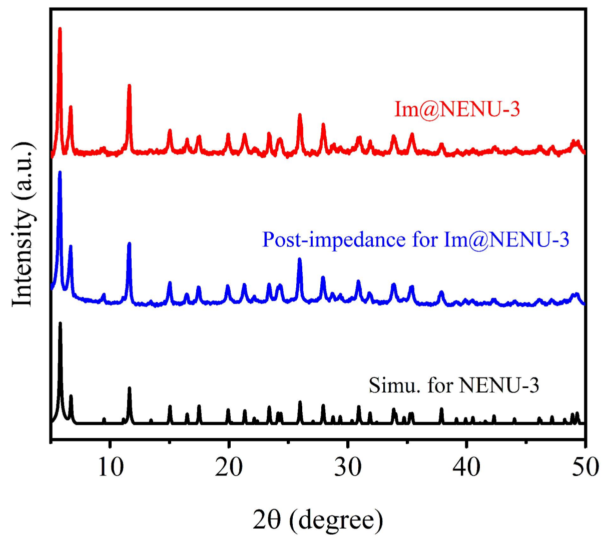

Fig. S7 PXRD patterns of post-impedance for Im@NENU-3.

The PXRD patterns of Im@NENU-3 samples before and after impedance testing are nearly identical, manifesting that Im@NENU-3 still maintains its structural integrity and crystallinity after AC impedance measurement. Therefore, Im@NENU-3 possesses excellent structural stability.

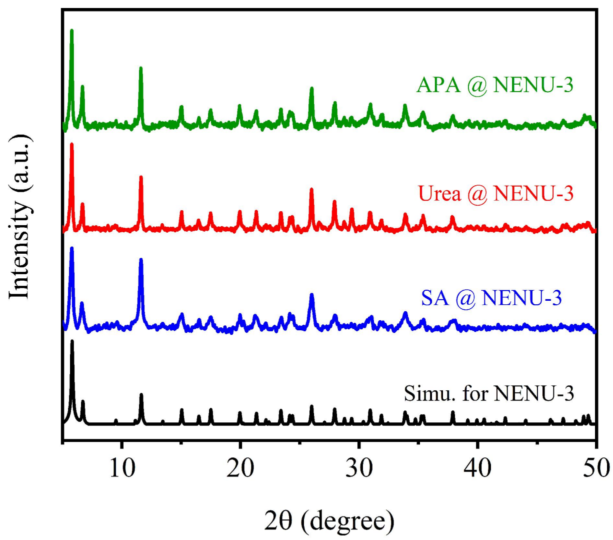

Fig. S8 PXRD patterns of APA@NENU-3, Urea@NENU-3 and SA@NENU-3.

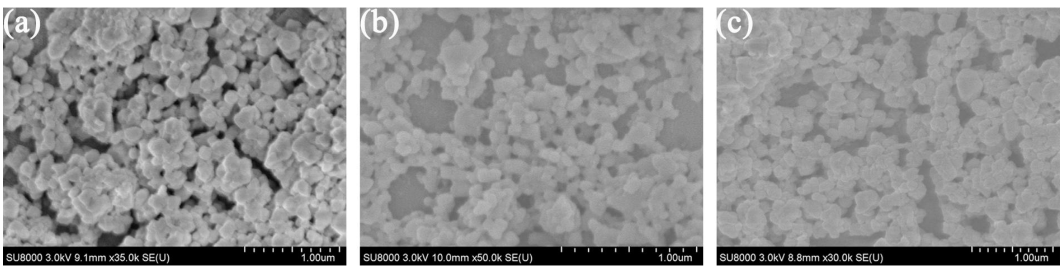

Fig. S9 SEM images of (a) APA@NENU-3, (b) Urea@NENU-3 and (c) SA@NENU-3.

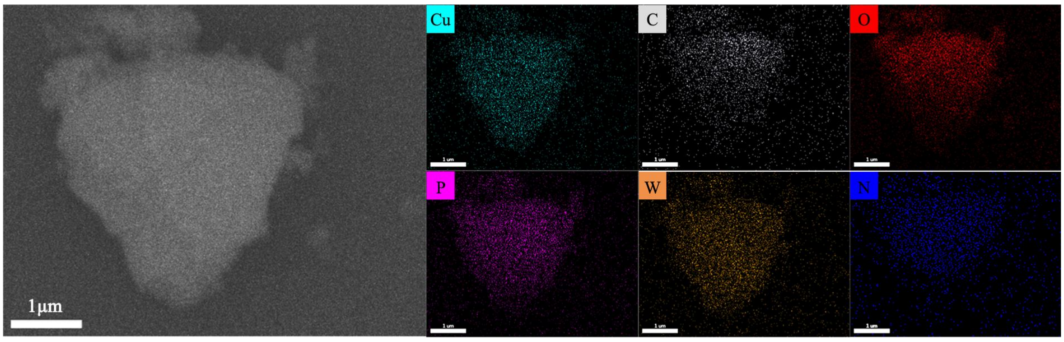

Fig. S10 SEM image and corresponding elemental mappings of APA@NENU-3

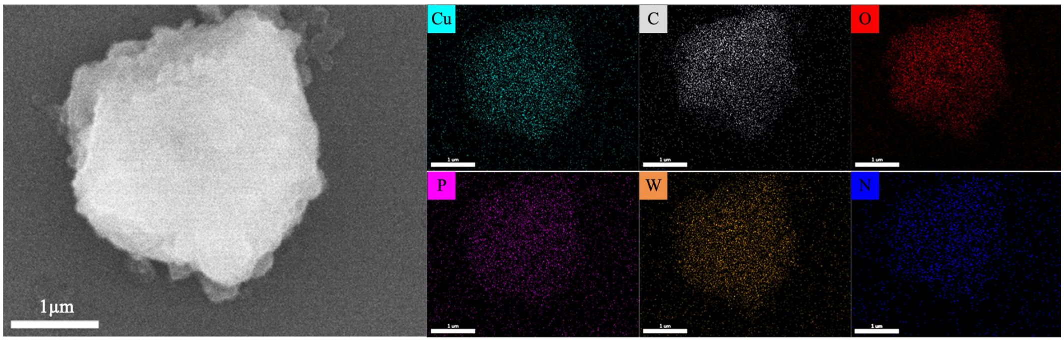

Fig. S11 SEM image and corresponding elemental mappings of Urea@NENU-3

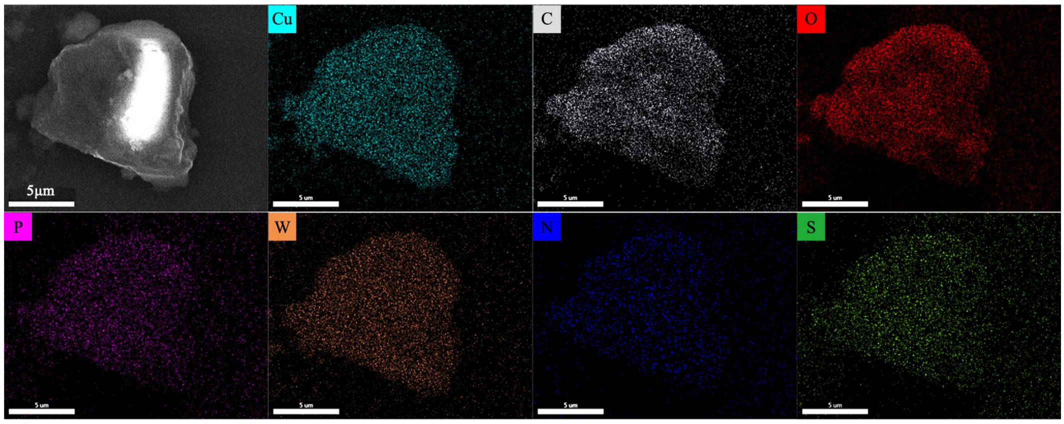

Fig. S12 SEM image and corresponding elemental mappings of SA@NENU-3

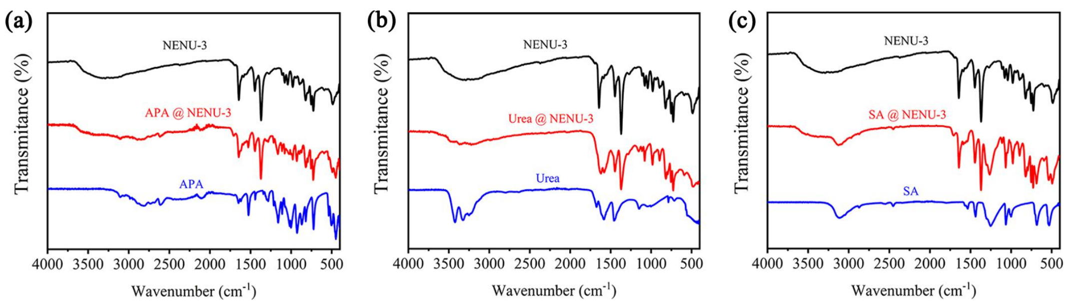

Fig. S13 FT-IR spectra of (a) APA@NENU-3, (b) Urea@NENU-3 and (c) SA@NENU-3

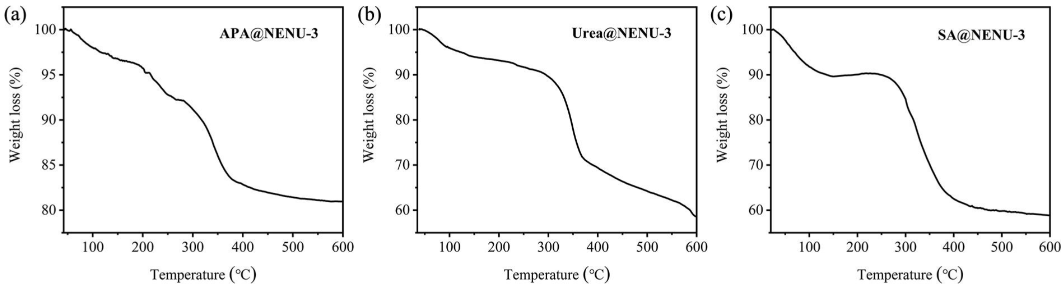

Fig. S14 TG plots of (a) APA@NENU-3, (b) Urea@NENU-3 and (c) SA@NENU-3.

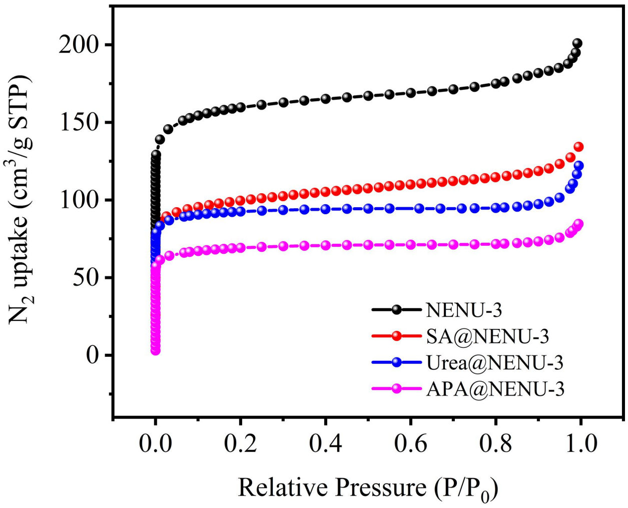

Fig. S15 N_2 adsorption isotherms of (a) APA@NENU-3, (b) Urea@NENU-3 and (c) SA@NENU-3.

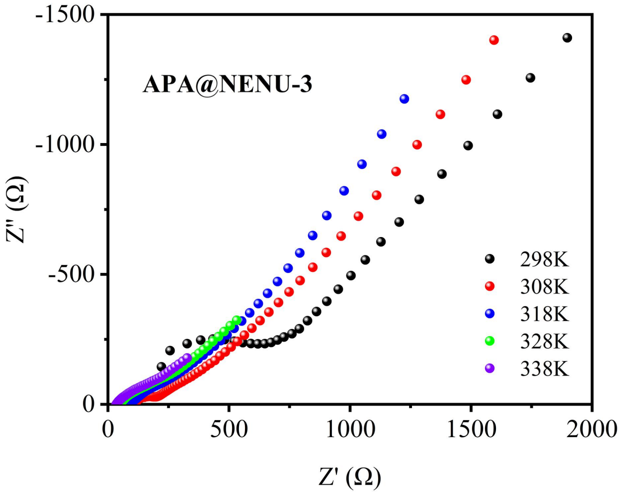

Fig. S16 Nyquist plots of APA@NENU-3 at different temperatures and 95% RH.

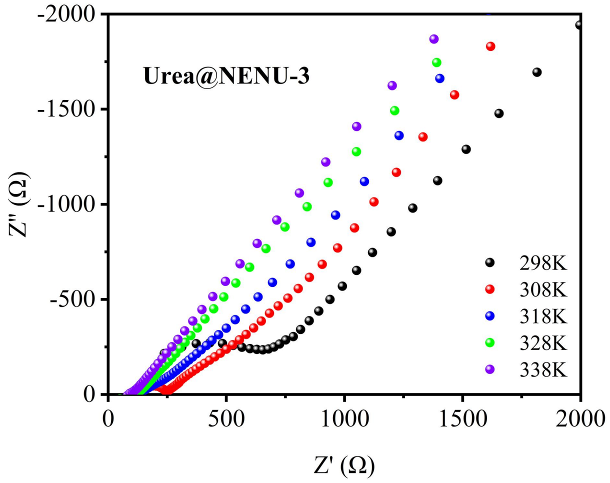

Fig. S17 Nyquist plots of Urea@NENU-3 at different temperatures and 95% RH.

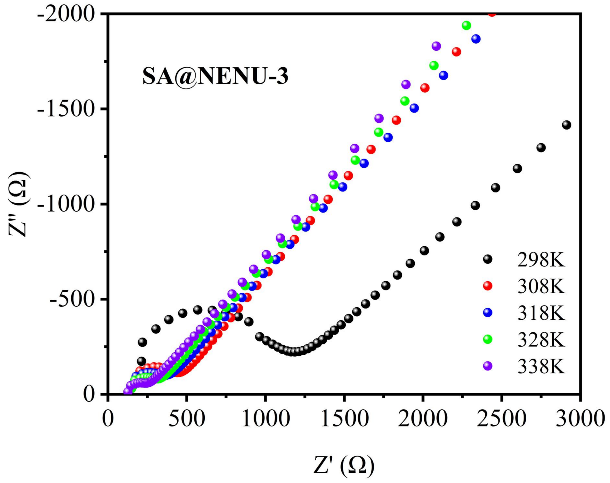

Fig. S18 Nyquist plots of SA@NENU-3 at different temperatures and 95% RH.

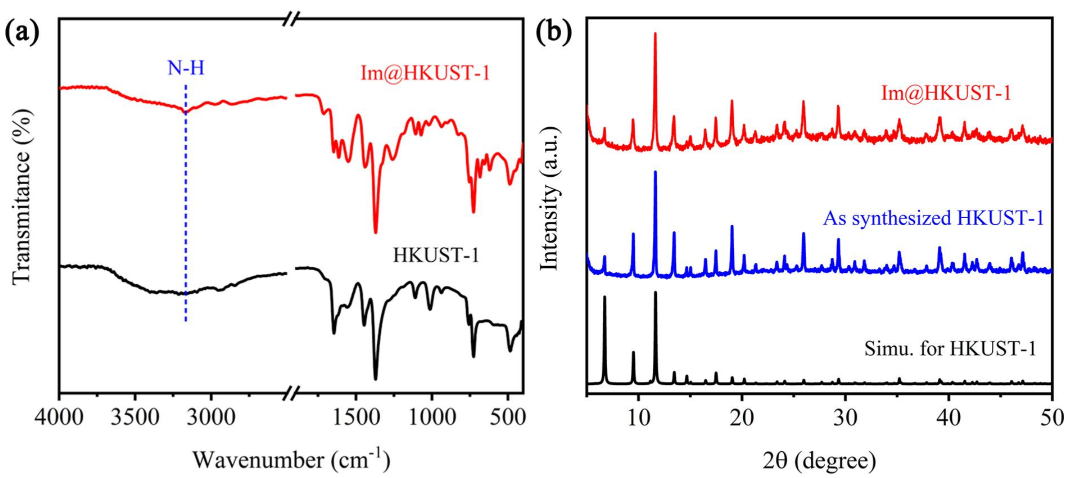

Fig. S19 FT-IR spectra and PXRD pattern of Im@HKUST-1.

The N-H stretching vibration peak is observed in the FT-IR spectrum of Im@HKUST-1 (Fig. S19a), suggesting that Im was successfully encapsulated into the pores of HKUST-1. The PXRD pattern of Im@HKUST-1 matches well with that of simulated HKUST-1 (Fig. S19b), revealing that it has the same framework structure with HKUST-1. And, no diffraction peaks of Im are observed, suggesting that Im was encapsulated into the pores of HKUST-1 and during the synthetic process no aggregated Im particles were formed.

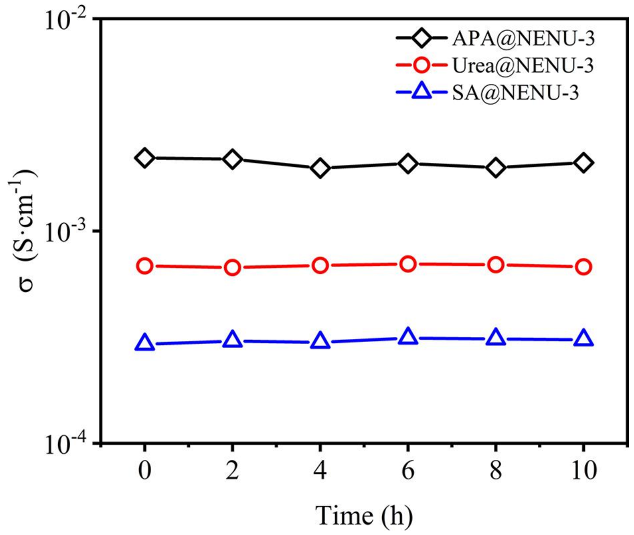

Fig. S20 Time-dependent proton conductivity of APA@NENU-3, Urea@NENU-3 and SA@NENU-3 at 338K and 95%RH

The proton conductivity of APA@NENU-3, Urea@NENU-3 and SA@NENU-3 can maintain at least 10 h, so Im@NENU-3 possesses excellent proton-conducting durability.

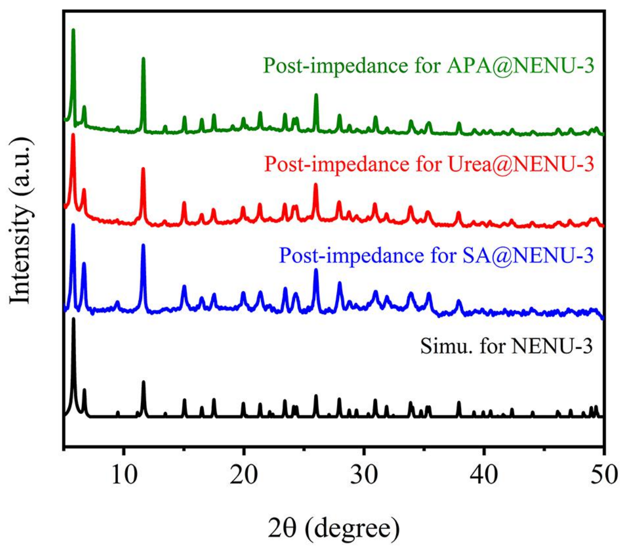

Fig. S21 PXRD patterns of post-impedance for APA@NENU-3, Urea@NENU-3 and SA@NENU-3.

The PXRD patterns of post-impedance for APA@NENU-3, Urea@NENU-3 and SA@NENU-3 are nearly identical to NENU-3, manifesting that they still maintain structural integrity and crystallinity after AC impedance measurement, so they all have excellent structural stability.

Section S3 Additional Tables

Table S1 Comparison of proton conductivity of Im@NENU-3 with some other representative proton conductors measured under hydrous condition.

Compounds	**Conductivity (S cm^{-1}) with measure conditions**	**References**
Fe-CAT-5	5.0×10^{-2} S cm^{-1} (298K, 98%RH)	1
H^+@Ni_2(dobdc) pH=1.8	2.2×10^{-2} S cm^{-1} (353K, 95%RH)	2
PCMOF2½	2.1×10^{-2} S cm^{-1} (358K, 90%RH)	3
Im@NENU-3	**7.06×10^{-3} S cm^{-1} (338K, 95 % RH)**	**This work**
TEPA@ZIF-8-H_2CO_3	5.38×10^{-3} S cm^{-1} (333 K, 99% RH)	4
$[Zn(L)Cl]_n$	4.72×10^{-3} S cm^{-1} (373K, 98 % RH)	5
PCMOF21-AcO	3.08×10^{-3} S cm^{-1} (358K, 95 % RH)	6
$[Cu(p\text{-IPhHIDC})]_n$	1.51×10^{-3} S cm^{-1} (373K, 98 % RH)	7
$[Zn(p\text{-IPhHIDC})]_n$	1.9×10^{-3} S cm^{-1} (373K, 98 % RH)	8
$[Co(p\text{-IPhHIDC})]_n$	1.07×10^{-3} S cm^{-1} (373K, 98 % RH)	8
$\{[Gd(L)(O_x)(H_2O)]_n \cdot 3H_2O\}$	4.7×10^{-4} S cm^{-1} (353K, 95 % RH)	9
Im@Eu-MOF	4.53×10^{-4} S cm^{-1} (348K, 98 % RH)	10
$\{[Dy(L)(O_x)(H_2O)]_n \cdot 1.5H_2O\}$	9.06×10^{-5} S cm^{-1} (353K, 95 % RH)	9
$\{[Mn(o\text{-CPhH}_2\text{IDC})(4.4'\text{-bipy})_{0.5}(H_2O)_2]\cdot 3H_2O\}_n$	5.74×10^{-5} S cm^{-1} (373K, 98 % RH)	11
$\{[Zn_5(o\text{-CPhH}_2\text{IDC})_2(o\text{-CPhHIDC})_2(2.2'\text{-bipy})_5]\cdot 5H_2O\}_n$	5.00×10^{-5} S cm^{-1} (373K, 98 % RH)	11
$[Cu_{12}(MES)_6(H_2O)_3]_n$	3.63×10^{-5} S cm^{-1} (333 K, 98% RH)	12
$\{[Cu_{12}(MPS)_6(H_2O)_4]\cdot 6H_2O\}_n$	2.75×10^{-5} S cm^{-1} (333 K, 98% RH)	12

References

1 N. T. Nguyen, H. Furukawa, F. Gandara, C. A. Trickett, H. M. Jeong, K. E. Cordova and O. M. Yaghi, *J. Am. Chem. Soc.*, 2015, **137**, 15394.

2 W. J. Phang, W. R. Lee, K. Yoo, D. W. Ryu, B. Kim and C. S. Hong, *Angew. Chem.*, 2014, **53**, 8383.

3 S. Kim, K. W. Dawson, B. S. Gelfand, J. M. Taylor and G. K. Shimizu, *J. Am. Chem. Soc.*, 2013, **135**, 963.

4 Q. Ren, J. W. Yu, H. B. Luo, J. Zhang, L. Wang and X. M. Ren, *Inorg. Chem.*, 2019, **58**, 14693.

5 Z. Q. Shi, N. N. Ji, M. H. Wang and G. Li, *Inorg. Chem.*, 2020, **59**, 4781.

6 D. A. Levenson, J. Zhang, B. S. Gelfand, S. P. Kammampata, V. Thangadurai and G. K. H. Shimizu, *Dalton Trans.*, 2020, **49**, 4022.

7 Z. Sun, S. Yu, L. Zhao, J. Wang, Z. Li and G. Li, *Chem. Eur. J.*, 2018, **24**, 10829.

8 Y. Qin, M.-H. Xue, B.-H. Dou, Z.-B. Sun and G. Li, *New J. Chem.*, 2020, **44**, 2741.

9 S. Biswas, J. Chakraborty, V. Singh Parmar, S. P. Bera, N. Ganguli and S. Konar, *Inorg. Chem.*, 2017, **56**, 4956.

10 S. F. Zhou, B. B. Hao, T. Lin, C. X. Zhang and Q. L. Wang, *Dalton Trans.*, 2020, **49**, 14490.

11 Y. Qin, Y. Li, K. Guo, H. Tang, L. Hou and G. Li, *New J. Chem.*, 2019, **43**, 4859.

12 J. M. Li, T. Y. Xu, Y. L. Zhao, X. L. Hu and K. H. He, *Dalton Trans.*, 2021, **50**, 7484.